TAO, Vol. 10, No. 1, 225-238, March 1999

High-resolution Carbonate Stratigraphy of IMAGES Core MD972151 from South China Sea

Chi-Yue Huang[1], Chia-Chun Wang[1] and Meixun Zhao[2]

(Manuscript received 24 November 1998, in final form 19 January 1999)

ABSTRACT

High-resolution carbonate stratigraphy of the deep-sea core MD972151 from the southwestern South China Sea shows millennial-scale variability similar to oxygen isotopic fluctuations recorded in ice cores from Greenland. In a long term of glacial-interglacial scale, carbonate contents in the interglacial time (up to 25 % by weight) were higher than that in the glacial periods (5-15 % by weight). Even for the last glacial, carbonate contents are relatively high in the interstadial events and low in the stadial horizons. This demonstrates clearly that carbonate content in the continental slope above the lysocline in the southwestern South China Sea is primarily controlled by dilution of terrigenous inputs, which in turn is due to sea-level fluctuations in response to changes of ice volume in high latitude regions.

(Key words: South China Sea, Carbonate stratigraphy, Ice volume, Terrigenous input)

1. INTRODUCTION

The South China Sea (SCS; 5°-22°N, 109°-121°E) is the largest marginal sea off the Asian continent (Figure 1). The SCS spread in NE-SW and E-W directions in late Oligocene - middle Miocene (Taylor and Hayes, 1983). This has resulted in the rhombic shape of the SCS. Wide passive continental shelves exist off Chinese coast (65 x 10^4 km^2) in the north and on the Sunda Shelf (115 x 10^4 km^2) off the Indochina Peninsula in the southwest. The Central Basin (80 x 10^4 km^2, > 4000 m) is below the present carbonate compensation depth (CCD; Figure 1). To the east, the SCS oceanic crust is subducting beneath the Philippine Sea plate along the Manila trench. In this geological context, the SCS marginal sea is a semi-closed marginal sea bounded by the landmasses of SE China to the north, the Indochina Peninsula to the west, the micro-continent of the Kalimantan-Palawan islands to the south, and the Luzon-Taiwan islands to the east (Figure 1).

The SCS exchanges its surface water with other water masses through several water gates.

[1] Department of Geology, National Taiwan University, Taipei, Taiwan, ROC
[2] Department of Earth Sciences, Dartmouth College, Hanover, NH 03755, USA

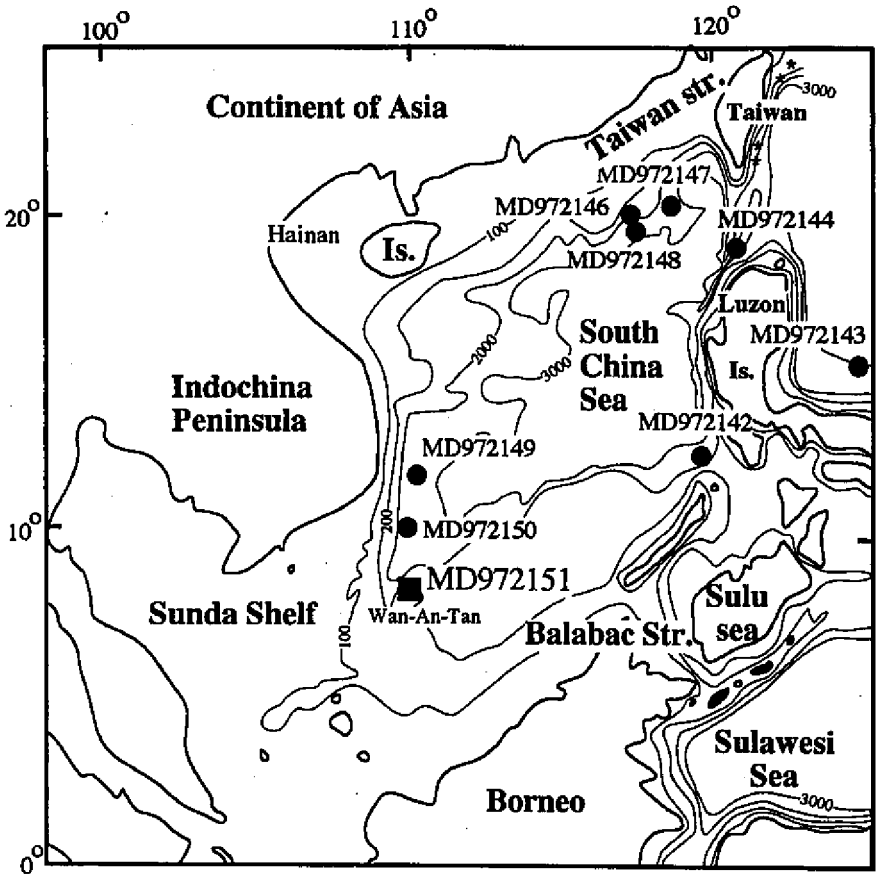

Fig. 1. Physiography of the South China Sea showing locations of seven deep sea cores obtained during IMAGES III/MD106 cruise.■: site of the studied core MD972151.

For example, the Indian Ocean surface water flows in the SCS through the Sunda Shelf in the summer, while the Chinese Coastal Water flows in the SCS through the Taiwan Strait in the winter. A branch of the Kuroshio Currents flows in the SCS through the southern part of the Luzon Strait off northern Luzon and then returns to join the main Kuroshio through the northern part of the Luzon Strait off southern Taiwan (Metzger and Hurlburt, 1996). In comparison, SCS surface water flows out to the Sulu sea through Mindoro and Balabac Straits (Figure 1). Sill depths of these water gates, however, are all shallow (less than 100 meters) except for the Luzon Strait. Therefore, during the last glacial time, when the global sea-level fell by more than 100 meters (Fairbanks, 1989), configuration of the SCS and water circulation would have been very different from the present one (Figure 2; Wang et al., 1995; Jian et al., 1998). However, the sill depth of the Luzon Strait is 2500 m, above which both surface and intermediate/deep waters of the SCS could exchange with the Pacific Ocean throughout the entire Quater-

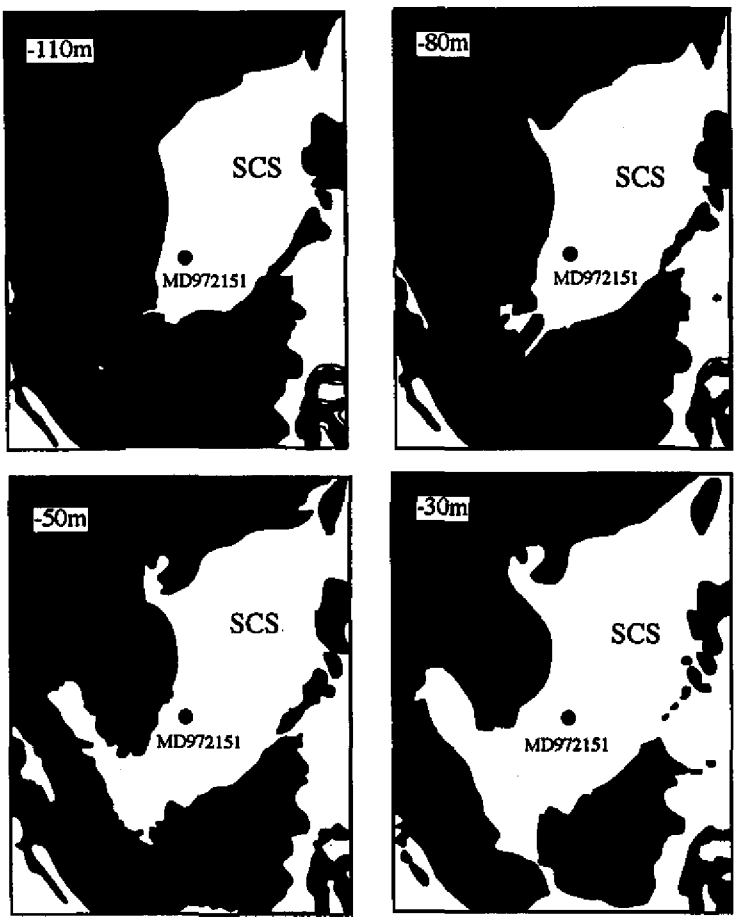

Fig. 2. Physiography of the South China Sea during progressive dropping of sea-level during the glacial period (after Jian et al., 1998).

nary.

Presently, climate and surface water circulation in the SCS marginal sea are controlled by seasonal reversal monsoon systems (Figure 3). During the summer monsoon season (May to September), when the warm Indian Ocean water invades the SCS through the Sunda Shelf, the SCS surface water flows from the southwest to northeast and sea surface temperature (SST) is homogeneously high (28-29°C). Local upwelling occurs off the coast of Vietnam (Figure 3). In contrast, during the winter monsoon season (October to April), the cold Chinese Coastal Water flows southward and the SCS surface water flows from the northeast to the southwest. The cold water, along with cold wind moving southward from the Siberian High Pressure, results in low SST and a steep temperature gradient in the SCS (21-24°C in the north and 25-27°C in the south). Previous studies have shown that on the Asian continent, weathering and precipitation have changed significantly in response to fluctuations of paleomonsoon systems

in the last 150 kyrs (An et al., 1990; Huang et al., 1997a; Liew et al., 1998). These changes will have further given rise to changes in the sedimentation rate of terrigenous materials along the SCS continental slope.

Sedimentation rate on the continental slope of the SCS is relatively high (10-60 cm/ky; Wang et al., 1995), which permits a high-resolution study of the IMAGES (International Marine Past Global Change Studies) goals. During Leg III of the IMAGES III (MD 106)-IPHIS cruise in June 1997, seven deep-sea cores were raised from the SCS (Figure 1). The purposes of this cruise across the SCS was to obtain high quality deep-sea cores for a high-resolution

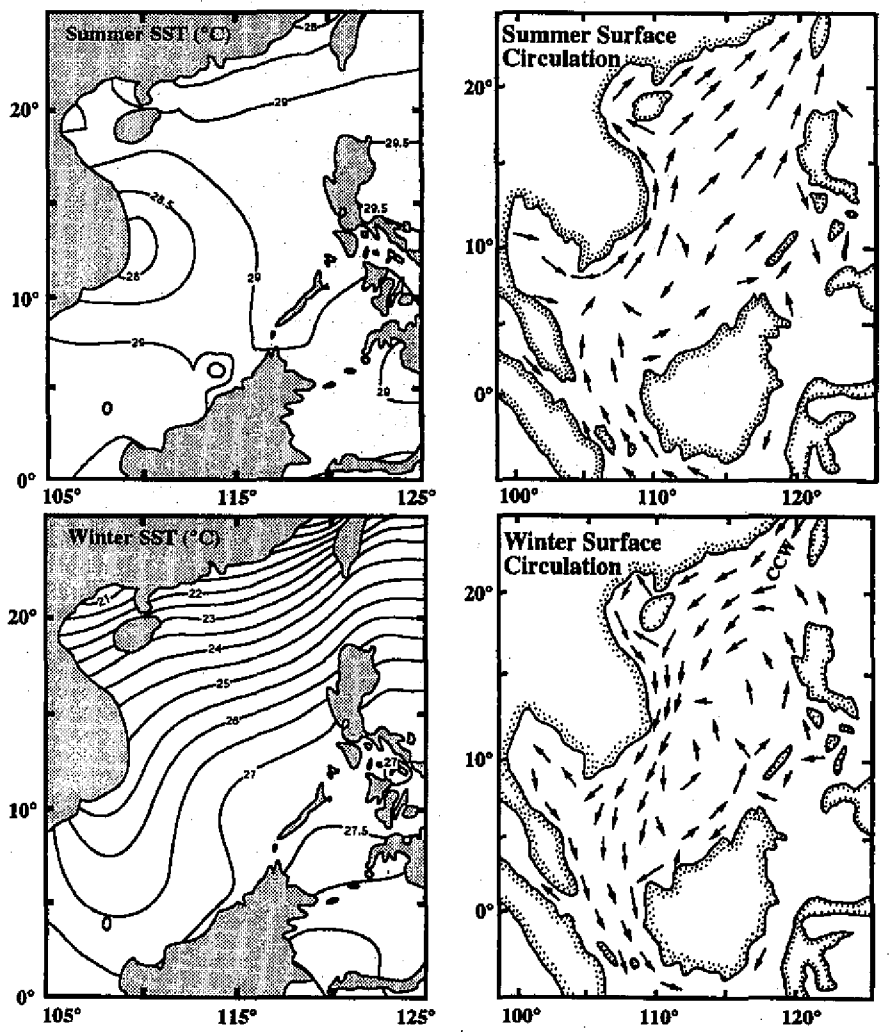

Fig. 3. Seasonal patterns of sea surface temperature and surface circulation of the South China Sea in summer and winter (after NOAA, 1994; Chen et al., 1985).

paleoceanography/paleomonsoon study in low latitude oceans and marginal seas. The results are then used to link with middle-high latitude paleoclimate records in the terrestrial loess sequences in central China and the Greenland ice cores as suggested in PAGES-PEP II (Chen et al., 1998; Huang and Chen, 1998). Here we present a high-resolution carbonate stratigraphy of the core MD972151 off Vietnam to construct a basic stratigraphy for a further detailed paleoclimatic correlation with Chinese loess and Greenland ice cores in the near future (Huang et. al., 1998).

2. CORE SITE LOCATION AND GENERAL OCEANOGRAPHY

The core MD972151 was taken from a water depth 1,598 m at 8°43.73'N, 109°52.17'E which is north of Wan-An-Tan, southeast off Vietnam (Figure 1). The site is on the continental slope to the east of the Sunda Shelf, where thick terrigenous sediments derived from the Indochina Peninsula and northern Kalimantan have accumulated (Figure 1). The core length is 26.72 m (down to Stage 6) with continuous and homogenous olive to dark clay. Some thin sandy layers occur in the lower part (>23 m, in Stage 6), which do not obviously disturb any significantly paleoclimatic signals registered in the core.

3. STUDY METHOD

Sediments 1-cm thick were sampled at 4-cm intervals, covering a 150-200 year time span. Carbonate content and TOC in freeze-dried sediments of the core MD972151 were determined by LECO WR-12 carbon analyzer at the Applied Geophysical Institute, NTOU, Keelung. Replicate analyses of the same samples gave a precision of better than 0.1 % for carbonate content. The age model is well established by multiple constraints: 12 AMS ^{14}C datings younger than 20 ka, oxygen isotope stratigraphy of *G. sacculifer* (Lee et al., 1999), Toba ash (71±5 ka; Ninkovich et al., 1978; Chesner et al., 1991; Zielinski et al., 1996; Schulz et al., 1998) at 1556-1558 cm, disappearance of pink *G. ruber* at 2171 cm (120 ka; Thompson et al., 1979) near MIS 5/6 boundary (Lee et al., 1999), and paleomagnetic Blake event in 2170-2320 cm (centered around120-130 ka; Lee, 1999). The carbonate data of core MD972151 are available electronically at Paleoceanographic Data Center of Core Laboratory-Center for Ocean Research, NSC, at the Institute of Applied Geophysics, National Taiwan Ocean University, Keelung, Taiwan, R.O.C. (Internet:http://140.121.175.114).

4. RESULTS

The carbonate stratigraphy (Table 1) of the core MD972151 plotted against depth and age are shown in Figure 4a and 4b. Carbonate content varies between 25 % and 3 % by weight over the whole length of the core as in the other cores from the SCS continental slope (Wang et al., 1995; Wang, 1998). In a long-term interglacial-glacial cycle, the carbonate curve is almost parallel to the oxygen isotope curve for planktic *G. sacculifer* (Lee et al., 1999) and

Table 1. Data for carbonate contents in the core MD972151.

Depth (cm)	CaCO3 (%)	Depth (cm)	CaCO3 (%)	Depth (cm)	CaCO3 (%)	Depth (cm)	CaCO3 (%)	Depth (cm)	CaCO3 (%
2.5	15.9	174.5	22.3	342.5	15.2	514.5	5.8	682.5	6.7
6.5	16.8	178.5	24.3	346.5	14.0	518.5	7.9	686.5	7.4
10.5	17.1	182.5	16.0	350.5	15.1	522.5	8.7	690.5	6.4
14.5	16.2	186.5	24.7	354.5	15.3	526.5	8.5	694.5	7.5
18.5	17.9	190.5	24.9	358.5	16.6	530.5	8.2	698.5	7.2
22.5	18.3	194.5	20.6	362.5	16.9	534.5	6.9	702.5	9.7
26.5	16.6	198.5	20.4	366.5	19.6	538.5	6.7	706.5	6.1
30.5	16.7	202.5	19.3	370.5	19.9	542.5	8.6	710.5	7.5
34.5	20.6	206.5	21.1	374.5	17.0	546.5	9.0	714.5	6.4
38.5	18.3	210.5	20.0	378.5	17.4	550.5	7.8	718.5	6.8
42.5	18.6	214.5	19.5	382.5	18.2	554.5	6.7	722.5	6.9
46.5	19.5	218.5	23.6	386.5	16.3	558.5	7.8	726.5	8.1
50.5	19.0	222.5	25.8	390.5	16.6	562.5	6.6	730.5	8.5
54.5	19.7	226.5	21.9	394.5	15.7	566.5	6.8	734.5	9.9
58.5	18.2	230.5	18.8	398.5	15.3	574.5	6.7	738.5	8.2
62.5	18.5	234.5	20.7	402.5	17.0	574.5	8.5	742.5	7.8
66.5	18.0	238.5	21.3	406.5	14.7	578.5	8.6	746.5	6.0
70.5	19.2	242.5	22.4	414.5	14.9	582.5	7.5	750.5	9.4
74.5	20.4	246.5	22.2	418.5	13.4	586.5	6.3	754.5	7.8
78.5	17.0	250.5	23.1	422.5	12.4	590.5	5.2	758.5	4.7
82.5	20.7	254.5	24.0	426.5	11.3	594.5	7.7	762.5	8.5
86.5	17.9	258.5	21.8	430.5	11.9	598.5	7.4	766.5	12.0
90.5	21.6	262.5	19.7	434.5	12.3	602.5	6.7	770.5	10.9
94.5	19.9	266.5	21.3	438.5	16.0	606.5	7.1	774.5	8.0
98.5	21.7	270.5	20.0	442.5	10.5	610.5	7.0	778.5	7.5
102.5	21.2	274.5	17.7	446.5	11.2	614.5	7.0	782.5	6.3
106.5	19.9	278.5	19.7	450.5	8.8	618.5	7.7	786.5	7.8
110.5	20.6	282.5	20.9	454.5	8.2	622.5	8.2	790.5	6.5
118.5	20.6	286.5	19.0	458.5	9.4	626.5	7.6	794.5	6.0
122.5	21.2	290.5	19.5	462.5	8.4	630.5	7.6	798.5	5.4
126.5	19.7	294.5	18.1	466.5	8.9	634.5	7.0	802.5	5.7
130.5	22.9	298.5	18.3	470.5	6.7	638.5	8.2	806.5	6.5
134.5	23.6	302.5	17.8	474.5	8.1	642.5	8.2	810.5	6.8
138.5	25.6	306.5	19.3	478.5	7.1	646.5	7.7	814.5	9.2
142.5	22.3	310.5	19.2	482.5	6.3	650.5	7.8	818.5	8.8
146.5	27.5	314.5	19.1	486.5	3.9	654.5	4.7	822.5	9.8
150.5	23.3	317.5	18.3	490.5	9.5	658.5	7.6	826.5	7.0
154.5	22.0	322.5	15.0	494.5	7.8	662.5	8.0	830.5	6.2
158.5	23.4	326.5	17.3	498.5	8.2	666.5	4.9	834.5	8.3
162.5	21.3	330.5	14.5	502.5	7.4	670.5	6.1	838.5	6.5
166.5	23.6	334.5	15.0	506.5	8.3	674.5	6.6	842.5	8.6
170.5	23.0	338.5	15.5	510.5	7.2	678.5	6.9	846.5	7.1

Table 1. continued.

Depth (cm)	CaCO3 (%)	Depth (cm)	CaCO3 (%)	Depth (cm)	CaCO3 (%)	Depth (cm)	CaCO3 (%)	Depth (cm)	CaCO3 (%)
850.5	8.1	1026.5	9.9	1220.0	10.8	1388.0	4.1	1556.0	0.3
854.5	7.2	1030.5	12.1	1224.0	9.3	1392.0	5.1	1560.0	7.8
858.5	8.1	1034.5	11.7	1228.0	12.3	1396.0	4.5	1564.0	7.9
862.5	6.5	1038.5	11.4	1232.0	10.2	1400.0	3.2	1568.0	8.2
866.5	9.7	1042.5	11.6	1236.0	12.0	1404.0	4.5	1572.0	4.8
870.5	7.7	1046.5	13.0	1240.0	7.5	1408.0	5.2	1576.0	10.5
874.5	8.9	1050.5	14.7	1244.0	11.3	1412.0	5.8	1584.0	7.8
878.5	8.1	1054.5	15.3	1248.0	9.9	1416.0	5.2	1588.0	8.4
882.5	9.0	1060.5	15.5	1252.0	13.8	1420.0	4.5	1592.0	7.5
886.5	6.5	1062.5	13.8	1256.0	7.9	1424.0	4.3	1596.0	10.3
890.5	6.9	1064.5	13.3	1260.0	10.1	1428.0	4.0	1600.0	12.1
894.5	9.4	1070.5	10.3	1264.0	9.5	1432.0	4.3	1604.0	11.7
902.5	11.3	1074.5	10.5	1268.0	10.5	1436.0	6.3	1608.0	14.8
906.5	13.4	1080.5	8.7	1272.0	8.5	1440.0	5.7	1612.0	13.1
914.5	12.3	1084.5	10.3	1276.0	8.4	1444.0	5.0	1616.0	11.7
918.5	14.1	1090.5	9.6	1280.0	6.9	1448.0	5.1	1620.0	12.5
922.5	10.2	1094.5	9.0	1284.0	6.5	1452.0	6.3	1624.0	16.0
926.5	9.9	1100.5	8.3	1288.0	5.4	1456.0	4.4	1628.0	10.1
930.5	8.9	1104.5	12.0	1292.0	8.1	1460.0	5.9	1632.0	18.2
934.5	8.4	1112.0	11.4	1296.0	6.6	1464.0	6.2	1636.0	16.4
938.5	5.0	1118.0	8.5	1300.0	7.1	1468.0	5.5	1640.0	17.5
942.5	7.5	1122.0	10.6	1304.0	4.8	1472.0	6.3	1644.0	13.9
946.5	4.7	1128.0	8.8	1308.0	6.1	1476.0	5.5	1648.0	14.2
950.5	10.5	1132.0	12.4	1312.0	7.8	1480.0	5.1	1652.0	10.2
954.5	5.9	1138.0	11.6	1316.0	5.2	1484.0	5.5	1656.0	12.2
958.5	8.5	1142.0	11.8	1320.0	4.6	1488.0	6.6	1660.0	13.1
962.5	6.3	1148.0	12.3	1324.0	4.0	1492.0	4.6	1664.0	10.5
966.5	5.3	1152.0	13.3	1328.0	8.5	1496.0	5.9	1668.0	10.7
970.5	7.8	1158.0	10.8	1332.0	6.6	1500.0	5.5	1672.0	10.4
974.5	10.5	1162.0	13.7	1336.0	4.8	1504.0	8.3	1676.0	11.3
978.5	10.1	1168.0	10.9	1340.0	7.3	1508.0	7.2	1680.0	8.1
982.5	9.8	1172.0	14.4	1344.0	4.8	1512.0	7.2	1684.0	10.8
986.5	12.2	1180.0	9.7	1348.0	4.0	1516.0	6.8	1688.0	10.0
990.5	9.0	1184.0	13.0	1352.0	3.5	1520.0	8.2	1692.0	7.8
994.5	10.1	1188.0	12.2	1356.0	4.6	1524.0	6.7	1696.0	7.5
998.5	10.4	1192.0	13.9	1360.0	8.9	1528.0	6.4	1700.0	7.9
1002.5	10.1	1196.0	11.9	1364.0	2.8	1532.0	5.5	1704.0	9.7
1006.5	12.7	1200.0	11.7	1368.0	6.8	1536.0	5.2	1704.0	8.7
1010.5	11.0	1204.0	8.5	1372.0	6.6	1540.0	5.6	1712.0	10.2
1014.5	12.2	1208.0	10.4	1376.0	5.5	1544.0	6.1	1716.0	11.9
1018.5	10.7	1212.0	9.3	1380.0	4.9	1548.0	4.7	1720.0	11.6
1022.5	8.8	1216.0	11.2	1384.0	4.9	1552.0	3.9	1724.0	11.8

Table 1. continued.

Depth (cm)	CaCO3 (%)	Depth (cm)	CaCO3 (%)	Depth (cm)	CaCO3 (%)	Depth (cm)	CaCO3 (%)	Depth (cm)	CaCO3 (%)
1728.0	11.5	1916.0	12.6	2104.0	23.3	2292.0	3.0	2478.0	5.2
1732.0	11.9	1920.0	12.5	2108.0	23.8	2296.0	4.2	2482.0	5.0
1736.0	12.3	1924.0	8.6	2112.0	23.2	2300.0	4.2	2486.0	4.3
1740.0	12.6	1928.0	9.5	2116.0	21.6	2304.0	3.3	2490.0	5.1
1744.0	9.9	1932.0	7.5	2124.0	24.1	2308.0	4.0	2494.0	5.3
1748.0	11.4	1936.0	9.0	2128.0	25.6	2312.0	2.7	2498.0	5.2
1752.0	9.1	1940.0	8.5	2132.0	22.3	2316.0	3.4	2502.0	4.2
1756.0	11.0	1944.0	8.5	2132.0	24.5	2322.0	3.8	2506.0	4.2
1760.0	10.0	1948.0	7.7	2136.0	24.1	2324.0	4.6	2510.0	4.0
1764.0	11.1	1952.0	8.4	2140.0	18.7	2328.0	3.2	2514.0	6.6
1768.0	10.3	1956.0	6.1	2144.0	21.4	2332.0	2.2	2518.0	5.2
1772.0	10.3	1960.0	8.6	2148.0	16.9	2336.0	3.0	2522.0	4.1
1776.0	10.6	1964.0	7.7	2152.0	16.2	2340.0	2.3	2526.0	5.6
1780.0	10.8	1968.0	8.3	2156.0	17.0	2344.0	3.0	2530.0	5.2
1788.0	9.7	1972.0	9.2	2160.0	17.6	2348.0	3.2	2534.0	3.6
1792.0	11.9	1976.0	9.3	2164.0	16.8	2352.0	3.1	2538.0	4.5
1796.0	12.8	1980.0	6.8	2168.0	19.3	2356.0	2.7	2542.0	6.2
1800.0	11.6	1984.0	9.4	2172.0	14.4	2360.0	3.1	2546.0	6.1
1804.0	13.6	1988.0	7.2	2176.0	15.8	2364.0	3.2	2550.0	6.9
1804.0	13.3	1992.0	8.1	2180.0	14.8	2368.0	3.9	2554.0	5.7
1808.0	13.2	1996.0	6.1	2184.0	16.5	2372.0	4.8	2558.0	4.4
1812.0	13.3	2000.0	5.5	2188.0	15.7	2376.0	3.1	2562.0	4.9
1816.0	14.8	2004.0	6.3	2192.0	16.2	2378.0	3.2	2566.0	6.0
1820.0	16.5	2008.0	4.3	2196.0	14.5	2382.0	3.3	2570.0	4.1
1824.0	14.3	2012.0	6.8	2200.0	16.2	2386.0	5.9	2574.0	4.4
1828.0	13.4	2016.0	5.8	2204.0	13.7	2390.0	4.1	2578.0	3.9
1832.0	14.1	2020.0	8.1	2208.0	9.5	2394.0	4.5	2582.0	3.9
1836.0	15.6	2024.0	6.9	2212.0	10.4	2398.0	2.9	2586.0	6.1
1840.0	19.3	2028.0	4.7	2216.0	10.1	2402.0	4.7	2590.0	2.7
1844.0	17.8	2032.0	8.2	2220.0	4.3	2406.0	5.8	2594.0	4.0
1848.0	17.2	2036.0	7.9	2224.0	7.8	2410.0	4.6	2598.0	4.8
1852.0	13.1	2040.0	9.8	2228.0	4.8	2414.0	6.3	2602.0	4.3
1856.0	20.0	2044.0	10.7	2232.0	2.5	2418.0	3.5	2606.0	3.1
1860.0	17.4	2048.0	13.4	2236.0	3.0	2422.0	4.7	2610.0	4.3
1864.0	21.4	2052.0	13.3	2240.0	5.5	2426.0	5.2	2614.0	8.3
1868.0	17.8	2056.0	11.6	2244.0	4.4	2430.0	3.7	2618.0	4.5
1872.0	18.4	2060.0	17.4	2248.0	3.9	2434.0	5.2	2622.0	4.0
1876.0	16.2	2064.0	13.9	2252.0	3.8	2438.0	4.5	2626.0	4.3
1880.0	17.7	2068.0	15.3	2256.0	3.6	2442.0	4.3	2630.0	3.2
1884.0	12.6	2072.0	16.3	2260.0	3.3	2446.0	4.7	2634.0	4.8
1888.0	15.1	2076.0	15.9	2264.0	4.6	2450.0	4.5	2638.0	4.7
1892.0	17.3	2080.0	15.6	2268.0	3.7	2454.0	3.9	2642.0	3.8
1896.0	14.5	2084.0	15.8	2272.0	3.4	2458.0	5.5	2646.0	4.4
1900.0	14.6	2088.0	15.7	2276.0	3.2	2462.0	6.2		
1904.0	16.8	2092.0	17.0	2280.0	3.9	2466.0	6.6		
1908.0	15.0	2096.0	19.8	2284.0	3.4	2470.0	5.7		
1912.0	14.4	2100.0	19.2	2288.0	4.0	2474.0	5.7		

SPECMAP. Carbonate contents are high (15-25%) in the interglacial (Stages 1 and 5) but low (3-15%) in the glacial intervals (Stages 2-3-4 and 6). The three intervals of high carbonate content in the lower part of the core (16-24 m) corresponding to Stage 5a (17%), 5c (21%) and 5e (25%), are intervened by two low intervals of Stage 5b (10%) and 5d (5%). However the carbonate content of these two lows in the last interglacial interval is still higher than that in the glacial intervals of Stage 4 (3-5%) above and Stage 6 (3%) below. Carbonate content in Stage 3 (8-15 %), especially in its early part, is higher than in Stage 2. In the upper part of the core, carbonate content rapidly increases from 5% in the LGM to 25% in the early Holocene, and then decreases to 15 % in the core top (938 years).

On a short-term millennial scale, carbonate content in MD972151 fluctuates at a high frequency (Figure 4b). Some events correlate with warm interstadial events found in the Greenland ice cores. For examples, the two peaks at 1520 and 1576 cm above and below the interval with the Toba eruption event of 1556-1558 cm correlate with IS 19 and 20 of GISP II, respectively (Schulz et al., 1998). The Toba eruption event is characterized by very low (<1 %) carbonate content. Carbonate peaks at 1252, 1172, 1060 and 906 cm are conspicuously higher than the interval below and above these peaks. These high carbonate peaks may correspond to IS 16, 14, 12 and 8, respectively, where alkenone sea surface temperature (U^{k}_{37}SST) are also relatively high (Huang et al., 1998). The low carbonate content in 322-362 cm corresponds to Younger Dryas where oxygen isotope values are relatively heavier (Lee et al., 1999). In comparison, high carbonate content at 362-370 cm correlates with Allerød warm event (14 Ka) of the GISP II ice core (Grootes, et al., 1993; Grootes and Stuiver, 1997). The carbonate data of core MD972151 are available electronically at Paleoceanographic Data Center of Core

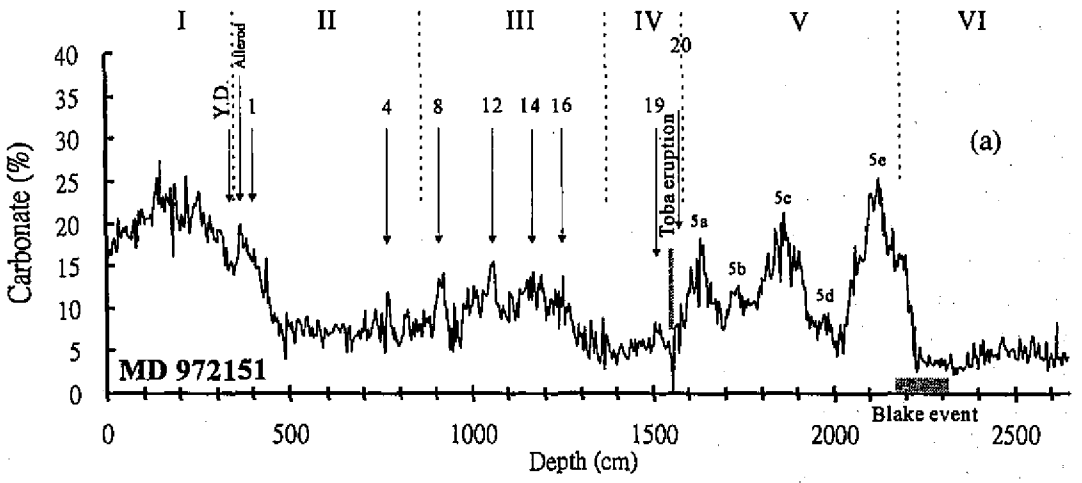

Fig. 4. Variations of carbonate content plotted against a) depth (cm) and b) age (ka) for the core MD972151. Lines with numbers are key horizons with high carbonate content correlated with interstadial events recorded in Greenland ice cores.

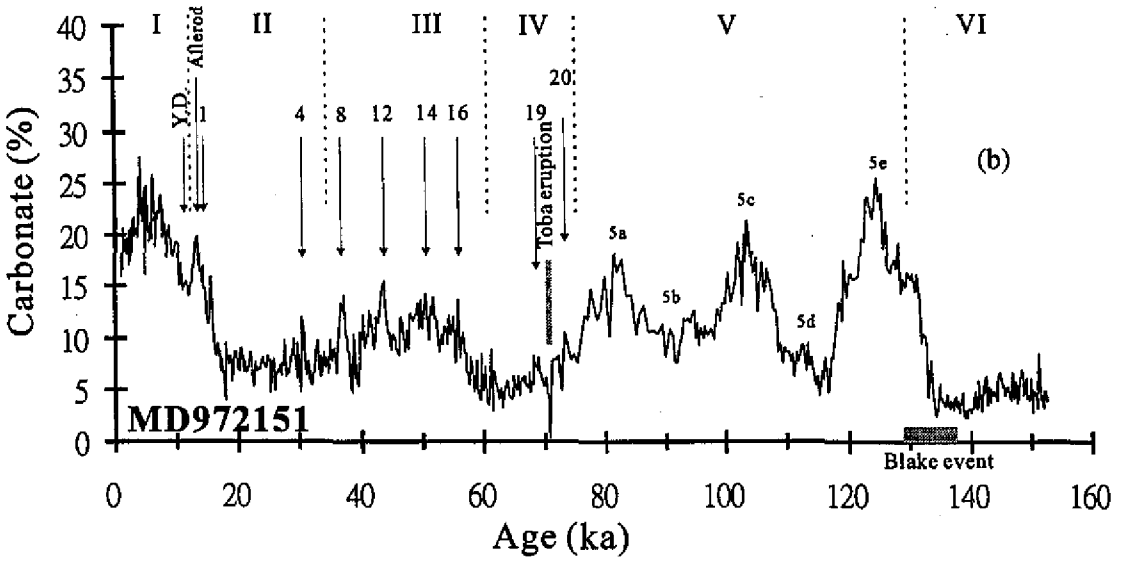

(*Fig. 4.* continued.)

Repository and Laboratory – National Center for Ocean Research, NSC, at the Institute of Applied Geophysics, National Taiwan Ocean University, Keelung, Taiwan, R. O. C. (Internet: http://140.121.175.114; cchuang@ntou66.ntou.edu.tw).

5. DISCUSSION

Carbonate content in marine environments is controlled by three factors: dissolution by corrosive bottom water, biological productivity in surface water, and dilution by terrigenous inputs.

Significant carbonate dissolution occurs below the carbonate lysocline, while carbonate is near zero or very low (< 3%) near the CCD (Berger, 1975; Bramlette, 1961). In the SCS, the depths of the lysocline and the CCD are about 3000 m and 3500 m, respectively (Rottmann, 1979). At present, the aragonite compensation depth (ACD) in the SCS is about 1000-1200 m. The core MD972151 is located at a water depth of 1598 m, which is below the ACD but far above the carbonate lysocline depth. In the last glacial, the ACD and CCD deepened to 2500 m and 4000 m, respectively (Thunell et al., 1992; Miao et al., 1994). Although there is no information about the carbonate lysocline in the glacial SCS, the depth of the carbonate lysocline in the glacial Pacific Ocean deepened as the ACD and CCD did (Farrell and Prell, 1989). An increase in the carbonate lysocline and CCD will have caused the biogenic carbonate fauna to be much better preserved (Wei et al., 1997; Chen et al., 1997) in the last glacial. Thus if dissolution is an important factor in controlling carbonate content of the core MD972151, the carbonate content in the last glacial interval should be greater than in the Holocene. However, this is not apparent in Figure 4. Therefore, dissolution is unlikely as a major factor controlling

carbonate content in MD972151.

Previous studies have suggested that surface productivity increased when the winter monsoon was enhanced in the last glacial (Thunell et al., 1992; Huang et al., 1997a, b). Moreover in the last glacial, a fall in sea-level led to the exposure of a wide continental shelf from which the SCS derived many nutrients. This would also have favored an increase in biological productivity, and thus would have increased the biogenic carbonate in the core. However in comparison to the interglacial intervals, carbonate contents in the last glacial were relatively low (Figure 4). Therefore, surface productivity is neither a major factor for controlling carbonate content in the study core.

Wide continental shelves (1,82 $x10^4$ km^2) occupy 52 % of the SCS's total area (350 $x10^4$ km^2). They exist off the Chinese coast (67 $x10^4$ km^2) in the north and off the Indochina Peninsula (Sunda Shelf,15 $x10^4$ km^2) in the southwest. At present, terrigenous sediments (**200 $x10^9$** Tons/year) derived from southern China are deposited on the northern shelf and slope via the Red River and Pearl River systems. Meanwhile, $160x10^9$ Tons of sediments are annually transported via the Mekong River system from the Tibetan Plateau, and then deposited on the Sunda Shelf and its slope (Milliman and Meade, 1983). These present data indicate that sedimentation in the SCS is greatly influenced by dilution of terrigenous inputs - the larger terrigenous inputs, the lower the carbonate content in the shelf-slope sediments. Furthermore, sea-level fluctuates in response to changes of ice volume. During an interglacial period, such as the present one, sea-level rises due to contraction of the ice volume in the high latitude regions. In contrast, during the glacial periods, expansion of the ice in high latitude regions causes a fall in sea-level and exposes the wide continental shelf. Thus much more terrigenous materials derived from both the continent and the exposed shelves, will be finally deposited on continental slope. This will strongly dilute biogenic carbonate components in the core MD972151 to as low as 3-5 % by weight in Stages 2-3-4 and 6. In comparison, during interglacial periods (sedimentation rate: Stage 1: 29.0 cm/kyrs and Stage 5: 10.6 cm/kyrs; Table 2), the Sunda Shelf was not exposed and even became a depositional site for the terrigenous sediments. Therefore, in the Stages 1 and 5 of the core MD972151 less continent-derived sediments were deposited on the continental slope and the carbonate content is relatively high. Similarly, the

Table 2. Sedimentation rate (cm/kyrs) for the core MD972151 based on multiple age constraints.

	Depth (cm)	Sedimentation rate (cm/kyrs)
Stage 1	0-350	29.0
Stage 2	350-862	21.8
Stage 3	862-1378	19.7
Stage 4	1378-1590	18.5
Stage 5	1590-2161	10.6
Stage 6	2161-2406	19.6

ice volume factor also plays a major role in controlling millennial-scale variations of carbonate content in interstadial-stadial cycles in the last glacial. Exposure of the continental shelf remains in balance with fluctuation of both sea-level and ice volume during the last glaciation. Much more of the shelf was exposed in the cool stadial event than in the warm interstadial event, and this led to a much lower carbonate content in the cool stadial events.

6. CONCLUSION

Using multiple age constraints, carbonate stratigraphy of the deep-sea core MD972151 shows millennial-scale fluctuations which correlate with D-O cycles found in the Greenland ice cores. Carbonate contents in the core MD972151 are primarily controlled by fluctuations of ice volume. During the glacial and cool stadial events of the last glacial, extensive glaciation in the high latitude regions resulted in a low sea-level which exposed the wide Sunda shelf, and thus provided much more of terrigenous sediments to dilute biological carbonate in the continental slope of the SCS. In contrast, during the interglacial periods and warm interstadial events of the last glacial, less glaciation in the Arctic, Greenland, and Antarctic regions resulted in a high sea-level, and therefore less terrestrial sediments were transported to the continental slope and thus carbonate contents were high.

Acknowledgements We appreciate assistance of the Captain and all cruise members on *Marion Dufresne* during the IMAGES III cruise in June 1997. This study and part of the IMAGES III (MD 106)-IPHIS cruise over the South China Sea (Leg III) were supported by the National Science Council, Republic of China under grants NSC86-2611-M-002-006 and NSC86-2611-M-002-04 to CY Huang. Project through grant NSC 88-2119-M-019-002.

REFERENCES

An, Z., G. Kukla, S. C. Porter and J. L. Xiao, 1990: The long-term paleomonsoon variation recorded by the loess-paleosol sequence in central China. *Quaternary International*, **7/8**, 91-95.

Berger, W. H., 1975: Deep-sea carbonates: Dissolution profiles from foraminiferal preservation. In: A. W. H. Be and W. H. Berger (Eds.), Dissolution Of Deep-Sea Carbonates, *Spec. Pub. Cushman Found. Foraminiferal Res.*, **13**, 82-86.

Bramlette, M. N., 1961: Pelagic sediments. In: M. Sears (Ed.), Oceanography. *Pub. Am. Assoc. Adv. Sci.*, **67**, 345-366.

Chen, M. T., C. Y. Huang and K. Y. Wei, 1997: 25,000-year late Quaternary records of carbonate preservation in the South China Sea. *Paleogeography, Paleoclimatology, Paleoecology*, **129**, 155-169.

Chen, M. T., L. Beaufort and the Shipboard Scientific Party of the IMAGES III /MD106-IPHIS Cruise (Leg III), 1998: Exploring Quaternary variability of the East Asian Monsoon, Kuroshio Current, and Western Pacific warm pool systems: High-resolution investigations of paleoceanography from the IMAGES III (MD106)-IPHIS cruise. *TAO*, **9**, 129-142.

Chen, S., T. Chen, X. Xu, Z. Chen and S. Sui, 1985: The Vast South China Sea. China Science Press, Beijing, 218 pp. (in Chinese)

Chesner, C. A., W. I. Rose, A. Deino, R. Drake and J. A. Westgate, 1991: Eruptive history of Earth's largest Quaternary caldera (Toba, Indonesia) clarified. *Geology*, **19**, 200-203.

Fairbanks, R. A., 1989: A 17,000 year glacio-eustatic sea-level record: Influence of glacial melting rates on the Younger Dryas event and deep sea circulation. *Nature*, **342**, 637-642.

Farrell, J. W. and W. L. Prell, 1989: Climatic changes and $CaCO_3$ preservation: An 800,000 year bathymetric reconstruction from the Central Equatorial Pacific Ocean. *Paleoceanography*, **4**, 447-466.

Grootes, P. M. and M. Stuiver, J. W. C. White, S. Johnsen, and J. Jouzel, 1993: Comparison of oxygen isotope records from the GISP2 and GRIP Greenland ice cores. *Nature*, **366**, 552-554.

Grootes, P. M. and M. Stuiver, 1997: Oxygen 18/16 variability in Greenland snow and ice with 10^{-3} to 10^{5}-year time resolution. *J. Geophy. Res.*, **102**, 26,455-26,470.

Huang, C. Y., P. M. Liew, M. Zhao, T. C. Chang, C. M. Kuo, M. T. Chen, C. H. Wang and L. F. Zheng, 1997a: Deep sea and lake records of the Southeast Asian paleomonsoons for the last 25 thousand years. *Earth and Planetary Sci. Lett.*, **146**, 59-72.

Huang, C. Y., S. F. Wu, M. Zhao, M. T. Chen, C. H. Wang, X. Tu and P. B. Yuan, 1997b: Surface ocean and monsoon climate variability in the South China Sea since the last glaciation. *Marine Micropaleontology*, **32**, 71-94.

Huang, C. Y. and M. T. Chen, 1998: Introduction to Taiwan IMAGES. *National Science Council Monthly*, **26**, 1291-1303.

Huang, C. Y., M. Zhao, C. C. Wang and W. C. Fan, 1998: A millennial-scale record of Asian paleomonsoon variability in the last 130 kyrs using South China Sea cores. *EOS*, **79**, F503.

Jian, Z., M. Chen, H. Lin and P. Wang, 1998: Stepwise paleoceanographic changes during the last deglaciation in the southern South China Sea: Records of stable isotope and microfossils. *Sci. In China (Series D)*, **41**, 187-194.

Lee, M. Y., K. Y. Wei and Y. G. Chen, 1999: A high resolution oxygen isotope stratigraphy for the last 150,000 years in the southern South China Sea: Core MD972151. *TAO*, **10**, 239-254.

Lee, T. Q., 1999: Last 160 Ka Paleomagnetic Directional Secular Variation Record from Core MD972151, Southwestern South China Sea. *TAO*, **10**, 255-264.

Liew, P. M., C. M. Kuo, S. Y. Huang and M. H. Tseng, 1998: Vegetation change and terrestrial carbon storage in eastern Asia during the last glacial maximum as indicated by a new pollen record from central Taiwan. *Global and Planetary Change*, **16-17**, 85-94.

Metzger, E. J. and H. E. Hurlburt, 1996: Coupled dynamics of the South China Sea, the Sulu Sea, and the Pacific Ocean. *J. Geophys. Res.*, **101**, 12,331-12,352.

Miao, Q., R. C. Thunell and D. M. Anderson, 1994: Glacial-Holocene carbonate dissolution and sea surface temperature in the South China and Sulu Seas. *Paleoceanography*, **9**, 269-290.

Milliman, J. D. and R. H. Meade, 1983: World-wide delivery of river sediment to the ocean.

J. Geology, **91**, 1-21.

Ninkovich, D., N. J. Shackleton, A. A. Abdel-Monem, J. D. Obradovich and G. Izett, 1978: K-Ar age of the Pleistocene eruption of Toba, north Sumatra. *Nature*, **276**, 574-577.

Rottmann, M. L., 1979: Dissolution of planktonic foraminifera and pteropods in South China Sea sediments. *J. Foraminiferal Res.*, **9**, 41-49.

Schulz, H., U. von Rad and H. Erlenkeuser, 1998: Correlation between Arabian Sea and Greenland climate oscillations of the past 110,000 years. *Nature*, **393**, 54-57.

Taylor, B. and D. E. Hayes, 1983: Origin and history of South China Sea Basin. In: D. E. Hayes (Ed.), The Tectonic and Geological Evolution of Southeast Asian Seas and Islands, Part 2. Am. Geophys. Union, Geophys. Monogr., Ser. 27, 23-56.

Thunell, R. C., Q. Miao, S. E. Calvert and T. F. Pedersen,1992: Glacial-Holocene biogenic sedimentation patterns in the South China Sea: Productivity variations and surface water pCO_2. *Paleoceanography*, **7**, 143-162.

Thompson, P. R., A. W. H. Be and J. C. Duplessy, 1979: Disappearance of pink-pigmented *Globigerionoides ruber* at 120,000 yr B. P. in the Indian and Pacific Oceans. *Nature*, **280**, 554-558.

Wang, P., L. Wang, Y. Bian and Z. Jian, 1995: Late Quaternary paleoceanography of the South China Sea. *Marine Geology*, **127**, 145-165.

Wang, P., 1998: Glacial carbonate cycles in Western Pacific marginal seas. *Marine Geology and Quaternary Geology*, **18**, 1-12 (in Chinese with English abstract).

Wei, K. Y., T. N. Yang and C. Y. Huang, 1997, Glacial-Holocene calcareous nannofossils and paleoceanography in the northern South China Sea. *Marine Micropaleontology*, **32**, 95-114.

Wyrtki, K., 1981: An estimate of equatorial upwelling in the Pacific. *Joural Physic. Oceanog.*, **11**, 1205-1214

Zielinski, G. A., P. A. Mayewski, L. D., Meeker, S. Whitlow, and M. S. Twicker, 1996: Potential atmospheric impact of the Toba meg-eruption ~ 71,000 years ago. *Geophysic. Res. Lett.*, **23**, 837-840.